

# Quantum Simulation for Partial Differential Equations with Physical Boundary or Interface Conditions

Shi Jin<sup>\*1,2</sup>, Xiantao Li<sup>†4</sup>, Nana Liu<sup>‡1, 2, 3</sup>, and Yue Yu<sup>§1</sup>

<sup>1</sup>School of Mathematical Sciences, Institute of Natural Sciences, MOE-LSC, Shanghai Jiao Tong University, Shanghai, 200240, P. R. China

<sup>2</sup>Shanghai Artificial Intelligence Laboratory, Shanghai, China

<sup>3</sup>University of Michigan-Shanghai Jiao Tong University Joint Institute, Shanghai 200240, China

<sup>4</sup>Department of Mathematics, The Pennsylvania State University, University Park, Pennsylvania 16802, USA

May 5, 2023

## Abstract

This paper explores the feasibility of quantum simulation for partial differential equations (PDEs) with physical boundary or interface conditions. Semi-discretisation of such problems does not necessarily yield Hamiltonian dynamics and even alters the Hamiltonian structure of the dynamics when boundary and interface conditions are included. This seemingly intractable issue can be resolved by using a recently introduced Schrödingerisation method [[JLY22a](#), [JLY22b](#)] – it converts any linear PDEs and ODEs with non-Hermitian dynamics to a system of Schrödinger equations, via the so-called warped phase transformation that maps the equation into one higher dimension. We implement this method for several typical problems, including the linear convection equation with inflow boundary conditions and the heat equation with Dirichlet and Neumann boundary conditions. For interface problems we study the (parabolic) Stefan problem, linear convection, and linear Liouville equations with discontinuous and even measure-valued coefficients. We perform numerical experiments to demonstrate the validity of this approach, which helps to bridge the gap between available quantum algorithms and computational models for classical and quantum dynamics with boundary and interface conditions.

**Keywords:** Schrödingerisation; Quantum simulation; Physical boundary conditions; Interface problems; Geometric optics problems

---

\*shijin-m@sjtu.edu.cn

†xxl12@psu.edu

‡nana.liu@quantumlah.org

§terenceyuyue@sjtu.edu.cn

# Contents

<b>1</b>	<b>Introduction</b>	<b>2</b>
<b>2</b>	<b>Quantum simulations via Schrödingerisation</b>	<b>4</b>
<b>3</b>	<b>Linear convection equation with inflow boundary conditions</b>	<b>7</b>
<b>4</b>	<b>Heat equation with Dirichlet or Neumann boundary conditions</b>	<b>9</b>
<b>5</b>	<b>Linear PDEs for interface problems</b>	<b>11</b>
5.1	The linear advection equation . . . . .	12
5.2	The Stefan problem . . . . .	13
<b>6</b>	<b>Geometric optics problems with partial transmissions and reflections</b>	<b>15</b>
6.1	The geometric optics problem . . . . .	16
6.1.1	The Hamilton-Jacobi equation for the geometric optics . . . . .	16
6.1.2	The Liouville representation for the Hamilton-Jacobi equation . . . . .	17
6.1.3	The condition for transmissions and reflections at the interface . . . . .	18
6.2	The Hamiltonian-preserving scheme . . . . .	19
6.2.1	The numerical flux . . . . .	19
6.2.2	The Schrödingerisation simulation . . . . .	21
<b>7</b>	<b>Conclusion</b>	<b>21</b>

## 1 Introduction

We consider the problem of quantum simulation for partial differential equations (PDEs) with physical boundary and interface conditions. In most practical applications, one often needs to solve PDEs in a bounded domain, in which boundary conditions should be provided for the problem to be solvable. Typical physical boundary conditions include Dirichlet, Neumann, and Robin (or mixed) conditions. One also encounters interface problems when the background media is heterogeneous, for example, waves propagation across different media, heat conduction through different materials, etc.

Numerically solving PDEs becomes challenging when the space dimension is high (for example the  $N$ -body Schrödinger equation, kinetic equations such as the Boltzmann equation), or when there are multiple time and space scales. These problems are often too big to be solvable for classical computers, and in recent years there are increasing activities in developing quantum algorithms that use quantum computers—yet to be developed in the future—to solve PDEs [CPP<sup>+</sup>13, Ber14, MP16, CJO19, ESP19, CL20, LMS20, CLO21, JL22, GJL22, JLY22c], many of which rely upon the exponential acceleration advantages in quantum linear systems of equations [HHL09, CKS17, CAS<sup>+</sup>21, Ber14, BCOW17, CL20, SS19]. One way to develop quantum PDE solvers is to first discretise the spatial variables to get a system of ordinary differential equations

(ODEs), which in turn is solved by quantum ODE solvers [Ber14, BCOW17, CL20]. In particular, when the resulting ODE is also a Hamiltonian system, one can perform quantum simulations with less time complexity than quantum ODE solvers or other quantum linear algebra solvers (e.g., the quantum difference methods [Ber14, JLY22c]). Thus the design of quantum simulation algorithms for solving linear PDEs become interesting and important. See a very recent proposal using block-encoding [ALWZ22].

In a recent work, a new, simple and generic framework coined as *Schrödingerisation* was introduced [JLY22a, JLY22b] that allows quantum simulation for *all* linear PDEs and ODEs, and even some iterative methods in linear algebra [JL23]. The idea is to use a warped phase transform that maps the equations to one higher dimension, which, in the Fourier space, become a system of Schrödinger’s equations! The method is extended to solve open quantum systems in a bounded domain where artificial boundary conditions –which are not unitary operators –are needed [JLLY23].

In this paper, we explore the Schrödingerisation technique for PDEs with physical boundary and interface conditions. These conditions do not have unitary properties thus are not naturally suitable for quantum simulations. While a (homogeneous) PDE, when spatially discretised, becomes a homogeneous system of ODEs or dynamical systems, the boundary conditions, when numerically discretised, could contribute to an inhomogeneous term in the dynamical system. Our idea, as laid out in [JLY22a, JLY22b], is to introduce an auxiliary variable such that the extended system becomes homogeneous again. Then one can adapt the Schrödingerisation technique to turn them into a Schrödinger or unitary system, thus allowing direct quantum simulation.

Interface conditions, on the other hand, need extra attention when solved numerically. These problems are often modeled by PDEs with discontinuous coefficients. The immersed interface methods [LL94, Pes02], which incorporate the physical interface conditions into the numerical fluxes, are among the most popular methods to numerically treat the interface conditions. In the case of wave propagation through heterogeneous media, Hamiltonian-Preserving schemes were proposed by Jin and Wen [JW05, JW06b], where the transmission and reflection of waves crossing the interface are naturally built into the numerical fluxes. We then solve the discretised system based on the above methods via Schrödingerisation.

We choose some prototype PDEs with boundary and interface conditions to showcase these methods. Among the PDEs we study include parabolic and convection equations, with Dirichlet and Neumann boundary conditions. For the interface problems, we study the (parabolic) Stefan problem, linear convection, and linear Liouville equations with discontinuous and even measure-valued coefficients.

The paper is organized as follows. In section 2 we briefly review the Schrödingerisation technique for linear dynamical systems. Section 2 studies linear convection equation with inflow (Dirichet) boundary conditions. In section 4 both Dirichlet and Neumann boundary conditions are considered. Section 5 studies linear convection and heat equations with discontinuous coefficients describing interfaces. In section 6 we study geometric optics problems across interfaces where the numerical fluxes need to take into account the partial transmissions and reflections. The paper is concluded in Section 7.

## 2 Quantum simulations via Schrödingerisation

Of central importance in quantum computing algorithms is Hamiltonian simulation techniques. Assuming access to a Hermitian matrix  $H$ , they construct a quantum circuit that implements the unitary operator  $U = \exp(-itH)$ . Equivalently, it provides a route to evolve the time-dependent Schrödinger equation,

$$i\partial_t\psi = H\psi. \quad (2.1)$$

More generally, one can simulate the unitary evolution driven by a time-dependent Hamiltonian  $H(t)$  [LW18]. The Schrödingerisation technique [JLY22a, JLY22b] extends Hamiltonian simulation methods to the solution of PDEs. The technique turns a general dynamical system into a (decoupled) system of Schrödinger equations, thus paving the way to solve general time-dependent PDEs using Hamiltonian simulation techniques. In this section, we review the main steps in the Schrödingerisation procedure.

In practice, a PDE in a physical domain can be first discretised in space, while keeping the continuous dependence on time. A wide variety of methods are available for this purpose, including finite difference methods, finite element elements, spectral methods, etc. Such a spatial discretisation strategy reduces the problem to an ODE system, which can be expressed in the following general form,

$$\begin{cases} \frac{d\mathbf{u}(t)}{dt} = A(t)\mathbf{u}(t) + \mathbf{b}(t), \\ \mathbf{u}(0) = \mathbf{u}_0, \end{cases} \quad (2.2)$$

where  $\mathbf{u}, \mathbf{b} \in \mathbb{C}^n$  and  $A \in \mathbb{C}^{n \times n}$ . In general,  $A$  is non-Hermitian, i.e.,  $A^\dagger \neq A$ , where "†" denotes conjugate transpose. We first show that it suffices to assume that  $\mathbf{b}(t) = \mathbf{0}$ . Otherwise one can instead consider the augmented system:

$$\begin{cases} \frac{d\mathbf{u}(t)}{dt} = A\mathbf{u}(t) + \mathbf{b}(t)v, & \mathbf{u}(0) = \mathbf{u}_0, \\ v_t = 0, & v(0) = 1, \end{cases}$$

where the second equation gives  $v(t) \equiv 1$ , which leads to the original ODE system. The above ODEs can be written in the following compact form

$$\begin{cases} \frac{d\tilde{\mathbf{u}}(t)}{dt} = \tilde{A}\tilde{\mathbf{u}}(t) \\ \tilde{\mathbf{u}}(0) = \tilde{\mathbf{u}}_0 \end{cases}, \quad \tilde{\mathbf{u}} = \begin{bmatrix} \mathbf{u} \\ v \end{bmatrix}, \quad \tilde{A} = \begin{bmatrix} A & \mathbf{b}(t) \\ \mathbf{0}^T & 0 \end{bmatrix}, \quad \tilde{\mathbf{u}}_0 = \begin{bmatrix} \mathbf{u}_0 \\ 1 \end{bmatrix}, \quad (2.3)$$

where the zero vector  $\mathbf{0}$  has the same size as  $\mathbf{b}$ . For this reason, without loss of generality, we assume  $\mathbf{b} = \mathbf{0}$  in the following.

Now we return to the general form (2.2). We begin by decomposing  $A$  into a Hermitian term and an anti-Hermitian term:

$$A = H_1 + iH_2,$$

where

$$H_1 = \frac{A + A^\dagger}{2} = H_1^\dagger, \quad H_2 = \frac{A - A^\dagger}{2i} = H_2^\dagger.$$

A natural assumption is that (2.2) inherits the stability of the original PDE, in that the eigenvalues of  $A$  have non-positive real parts. The stability property implies that  $H_1$  is negative

semi-definite. Using the warped phase transformation  $\mathbf{v}(t, p) = e^{-p}\mathbf{u}(t)$  for  $p \geq 0$  and symmetrically extending the initial data to  $p < 0$ , the ODEs are then transformed to a system of linear convection equations [JLY22a, JLY22b]:

$$\begin{cases} \frac{d}{dt}\mathbf{v}(t, p) = A\mathbf{v}(t, p) = -H_1\partial_p\mathbf{v} + iH_2\mathbf{v}, \\ \mathbf{v}(0, p) = e^{-|p|}\mathbf{u}_0. \end{cases} \quad (2.4)$$

Let  $Q^{-1}H_1Q = \text{diag}(\lambda_1, \dots, \lambda_n)$  with  $\lambda_j \leq 0$  and define  $\tilde{\mathbf{v}} = Q^{-1}\mathbf{v}$ . When neglecting the imaginary part, one can find that the wave  $\tilde{\mathbf{v}}_j$  moves from right to left with speed  $s_j = |\lambda_j|$ .

For numerical implementation, it is natural and convenient to introduce  $\alpha = \alpha(p)$  in the initial data of (2.4) for  $p < 0$ :

$$\begin{cases} \frac{d}{dt}\mathbf{v}(t, p) = A\mathbf{v}(t, p) = -H_1\partial_p\mathbf{v} + iH_2\mathbf{v}, \\ \mathbf{v}(0, p) = e^{-\alpha|p|}\mathbf{u}_0. \end{cases} \quad (2.5)$$

To match the exact solution,  $\alpha(p) = 1$  is necessary for the region  $p > 0$ . In the  $p > 0$ -domain, we will truncate the domain at  $p = R$ , where  $R$  is sufficiently large such that  $e^{-R} \approx 0$ . We will choose a large  $\alpha$  for  $p < 0$  so the solution (see Fig. 1) will have a support within a relatively small domain. Since the wave  $\tilde{\mathbf{v}}_j$  moves to the left, one needs to choose the artificial boundary at  $p = L < 0$ , for  $|L|$  large enough such that  $\tilde{\mathbf{v}}_j$ , initially almost compact at  $[L_0, R]$ , will not reach the point  $p = L$  during the duration of the computation. This will allow to use periodic boundary condition in  $p$  for spectral approximation.

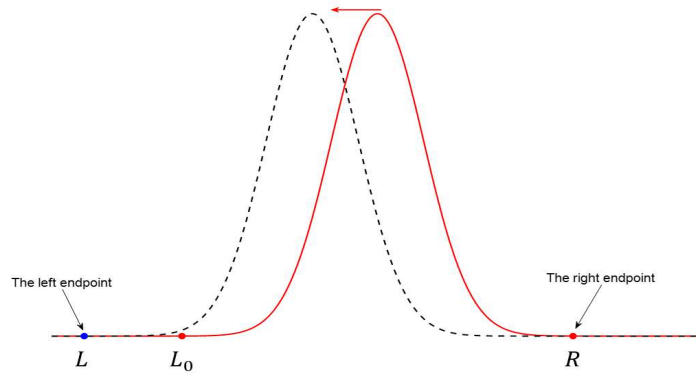


Fig. 1: Schematic diagram for the computational domain of  $p$

The solution  $\mathbf{u}(t)$  can be restored by

$$\mathbf{u}(t) = \int_0^\infty \mathbf{v}(t, p) dp \quad \text{or} \quad \mathbf{u}(t) = e^{p_k t} \mathbf{v}(t, p_k), \quad \text{for some } p_k > 0.$$

A more intuitive view is by discretising the  $p$  domain and concatenating the corresponding function for each  $p$ . Toward this end, we choose uniform mesh size  $\Delta p = (R-L)/N_p$  for the auxiliary variable with  $N_p$  being an even number, with the grid points denoted by  $a = p_0 < p_1 < \dots < p_{N_p} = b$ . Let the vector  $\mathbf{w}$  be the collection of the function  $\mathbf{v}$  at these grid points, defined more precisely as follows,

$$\mathbf{w} = [\mathbf{w}_1; \mathbf{w}_2; \dots; \mathbf{w}_n],$$

with “;” indicating the straightening of  $\{\mathbf{w}_i\}_{i \geq 1}$  into a column vector. This can also be expressed as a superposition state by  $|k\rangle$  as a new basis,

$$\mathbf{w}_i = \sum_k \mathbf{v}_i(t, p_k) |k\rangle.$$

By applying the discrete Fourier transformation in the  $p$  direction, one arrives at

$$\frac{d}{dt} \mathbf{w}(t) = -i(H_1 \otimes P_\mu) \mathbf{w} + i(H_2 \otimes I) \mathbf{w}. \quad (2.6)$$

At this point, we have successfully mapped the dynamics back to a Hamiltonian system. Here,  $P_\mu$  is the matrix expression of the momentum operator  $-i\partial_p$ , given by

$$P_\mu = \Phi D_\mu \Phi^{-1}, \quad D_\mu = \text{diag}(\mu_{-N_p/2}, \dots, \mu_{N_p/2-1}),$$

where  $\mu_l = 2\pi l / (R - L)$  are the Fourier modes and

$$\Phi = (\phi_{jl})_{M \times M} = (\phi_l(x_j))_{N_p \times N_p}, \quad \phi_l(x) = e^{i\mu_l(x-L)}.$$

By a change of variables  $\tilde{\mathbf{w}} = (I \otimes \Phi^{-1}) \mathbf{w}$ , one has

$$\frac{d}{dt} \tilde{\mathbf{w}}(t) = -i(H_1 \otimes D_\mu) \tilde{\mathbf{w}} + i(H_2 \otimes I) \tilde{\mathbf{w}}. \quad (2.7)$$

This is more amenable to an approximation by a quantum algorithm. In particular, if  $H_1$  and  $H_2$  are sparse, then (2.7) is a Schrödinger equation with the Hamiltonian  $H = H_1 \otimes D_\mu - H_2 \otimes I$  that inherits the sparsity.

With the state vector encoding  $\tilde{\mathbf{w}}$ , one can apply the quantum Fourier transform on  $p$  to get back to  $\mathbf{w}$  and then restore  $\mathbf{u}$  by projecting onto some basis  $|k\rangle$  or computing the observable induced by the numerical integration. See [JLY22a] for details on how to retrieve the quantum state with amplitudes proportional to  $\mathbf{u}$  and subsequently the observables.

This article aims to demonstrate the feasibility of quantum simulation for PDEs with physical boundary conditions and interface conditions. To assess the algorithm complexity associated with the implementation of the time-dependent Schrödinger equation, one can use the recent results by Berry et al. [BCS<sup>+</sup>20, Theorem 10], although the other algorithms can also be used for the assessment. Here we simply highlight the query complexity,

**Theorem 2.1.** *The TDSE (2.1) with an  $s$ -sparse Hamiltonian  $H(t)$  can be simulated from  $t = 0$  to  $t = T$  within error  $\epsilon$  with query complexity,*

$$\mathcal{O} \left( s \|H\|_{\max,1} \frac{\log(s \|H\|_{\max,1} / \epsilon)}{\log \log(\|H\|_{\max,1} / \epsilon)} \right). \quad (2.8)$$

Here the norm is defined as,

$$\|H\|_{\max,1} = \int_0^T \|H\|_{\max}(t) dt, \quad \|H\|_{\max}(t) := \max_{i,j} |H_{i,j}(t)|. \quad (2.9)$$

The strategy of implementing a semi-discrete approximation of a PDE system using Schrödingerisation is quite general. In the next few sections, we will illustrate how physical boundary conditions can be incorporated into this framework.

### 3 Linear convection equation with inflow boundary conditions

We first discuss how hyperbolic PDEs can be treated using the Schrödingerisation technique. As a specific example, we consider the quantum simulations for solving the first-order hyperbolic equation

$$u_t + \nabla \cdot (c(x)u) = 0, \quad \mathbf{x} = (x_1, x_2, \dots, x_d) \in (a, b)^d,$$

where  $c(x) = [c_1(x), c_2(x), \dots, c_d(x)]^T$  and  $u = u(t, x_1, x_2, \dots, x_d)$ . This is a typical linear wave equation through inhomogeneous media. It also appears in the linear representation of nonlinear dynamics, see the Liouville equation in [JL22, JLY23] for instance. For simplicity we set  $c_1(x) = \dots = c_d(x) \equiv 1$  in what follows and impose the inflow boundary conditions.

To construct a spatial discretisation, we introduce  $N_x + 1$  spatial mesh points  $0 < x_{i,0} < x_{i,1} < \dots < x_{i,N_x} = 1$  by  $x_{i,j} = a + j\Delta x$  in the  $x_i$ -direction, where  $\Delta x = (b - a)/N_x$ . Let  $\mathbf{j} = (j_1, j_2, \dots, j_d)$ . In addition, we consider the upwind scheme, which can be written as

$$\frac{d}{dt}u_{\mathbf{j}}(t) + \sum_{k=1}^d \frac{u_{\mathbf{j}}(t) - u_{\mathbf{j}-\mathbf{e}_k}(t)}{\Delta x} = 0, \quad (3.1)$$

where  $\mathbf{e}_k = (0, \dots, 0, 1, 0, \dots, 0)$  with  $k$ -th entry being 1 and  $j_k = 1, 2, \dots, N_x$  and we assume that the scheme is also applied to the right endpoint  $x = x_{i,N_x}$  along each dimension. Denote by  $\mathbf{u}$  the vector form of the  $d$ -order tensor  $(u_{\mathbf{j}}) = (u_{j_1, j_2, \dots, j_d})$ :

$$\mathbf{u} = \sum_{\mathbf{j}} u_{\mathbf{j}} |\mathbf{j}\rangle = \sum_{j_1, j_2, \dots, j_d=1}^{N_x} u_{j_1, j_2, \dots, j_d} |j_1, j_2, \dots, j_d\rangle,$$

where we have used the notation in quantum computation. One can refer to [JLY23] for details. The associated linear system can be represented as

$$\sum_{\mathbf{j}} \left( \frac{d}{dt}u_{\mathbf{j}}(t) + \sum_{k=1}^d \frac{u_{\mathbf{j}}(t) - u_{\mathbf{j}-\mathbf{e}_k}(t)}{\Delta x} \right) |\mathbf{j}\rangle = \mathbf{0}.$$

Due to the wave propagation nature of the PDE, the boundary conditions should only be imposed on one side of the boundaries. To write the above system in matrix form, let us assume that  $u_{\mathbf{j}}$  can be decomposed as  $u_{\mathbf{j}} = u_{j_1} u_{j_2} \dots u_{j_d}$ . Noting that  $u_{j_1, \dots, j_d}$  ( $j_k = 0$ ) are the given inflow boundary values in the  $x_k$ -direction, we have

$$\begin{aligned} \sum_{\mathbf{j}} u_{\mathbf{j}-\mathbf{e}_k} |\mathbf{j}\rangle &= \sum_{j_i=1, i \neq k}^{N_x} u_{j_1, \dots, 0, \dots, j_d} |j_1, \dots, 1, \dots, j_d\rangle \\ &+ \sum_{j_1=1}^{N_x} u_{j_1} |j_1\rangle \otimes \dots \otimes \sum_{j_k=2}^{N_x} u_{j_k-1} |j_k\rangle \otimes \dots \otimes \sum_{j_d=1}^{N_x} u_{j_d} |j_d\rangle \\ &=: \mathbf{u}_{0k} + \mathbf{u}^{(1)} \otimes \dots \otimes T_h \mathbf{u}^{(k)} \otimes \dots \otimes \mathbf{u}^{(d)} \\ &= \mathbf{u}_{0k} + (I \otimes \dots \otimes T_h \otimes \dots \otimes I) (\mathbf{u}^{(1)} \otimes \dots \otimes \mathbf{u}^{(d)}) \\ &= \mathbf{u}_{0k} + (I \otimes \dots \otimes T_h \otimes \dots \otimes I) \mathbf{u}, \end{aligned}$$

where

$$\mathbf{u}_{0k}(t) = \sum_{j_i=1, i \neq k}^{N_x} u_{j_1, \dots, 0, \dots, j_d} |j_1, \dots, 1, \dots, j_d\rangle \quad (0 \text{ and } 1 \text{ are located at the } k\text{-th position})$$

is the vector generated by left boundary values in the  $x_k$ -direction,

$$\mathbf{u}^{(i)} = \sum_{j_i=1}^{N_x} u_{j_i} |j_i\rangle, \quad i = 1, 2, \dots, d$$

and

$$T_h = \begin{bmatrix} 0 & & & & \\ 1 & \ddots & & & \\ & \ddots & \ddots & & \\ & & \ddots & \ddots & \\ & & & 1 & 0 \end{bmatrix}_{N_x \times N_x}. \quad (3.2)$$

We therefore obtain the system (2.2) with

$$A = \underbrace{L_h \otimes I \otimes \dots \otimes I}_{d \text{ matrices}} + \dots + I \otimes \dots \otimes L_h \otimes I + I \otimes I \otimes \dots \otimes L_h, \quad L_h = \frac{1}{\Delta x} (T_h - I). \quad (3.3)$$

and

$$\mathbf{b}(t) = \frac{1}{\Delta x} \sum_{k=1}^d \mathbf{u}_{0k}(t).$$

To test this approach, we consider the implementation in 1D. According to the introduction in Section 2, the underlying waves move from right to left with speed

$$s_j = -\lambda_j(H_1) = -\lambda_j\left(\frac{A + A^T}{2}\right) = \frac{2}{\Delta x} \sin^2 \frac{j\pi}{2(N_x + 1)}, \quad j = 1, 2, \dots, N_x$$

when  $\mathbf{b}(t) = \mathbf{0}$  is assumed. Let  $s_* = \max\{s_j\}$ . We know that the fastest left moving wave will have a speed  $s_* = \mathcal{O}(1/\Delta x)$ . Given the evolution time  $T$ , we can estimate a large enough  $|L|$  such that

$$s_* T \leq L_0 - L \quad \text{or} \quad L = L_0 - s_* T. \quad (3.4)$$

We use the backward Euler scheme for the temporal discretisation. It is important to note that the purpose of these experiments is to demonstrate that the equation (2.7) in the Schrödingerisation captures the dynamics under various physical boundary conditions. For higher dimensional problems, a quantum implementation of (2.7) is preferred to classical computers, due to the less dependence of the complexity on the dimension.

The initial and boundary values are chosen such that the exact solution is given by  $u(t, x) = e^{x-t}$ . Since the speed  $s_*$  scales as  $\mathcal{O}(1/\Delta x)$  (we take  $s_* = 2/\Delta x$ ), we choose a relatively large spatial domain  $[a, b] = [0, 10]$  such that  $|L|$  is not very large. In the numerical test, we choose  $T = 1$ ,  $L_0 = -1$ ,  $R = 10$  and  $\alpha(p) = 10$  for  $p < 0$ . For the spatial and  $p$  domains, we take  $N_x = N_p = 64$ , then the estimated  $L = -9.5333$ . We also take  $N_t = 100$  for the temporal discretisation. The result at  $t = T$  is displayed in Fig. 2, from which we observe the numerical solution is well matched with the exact one.

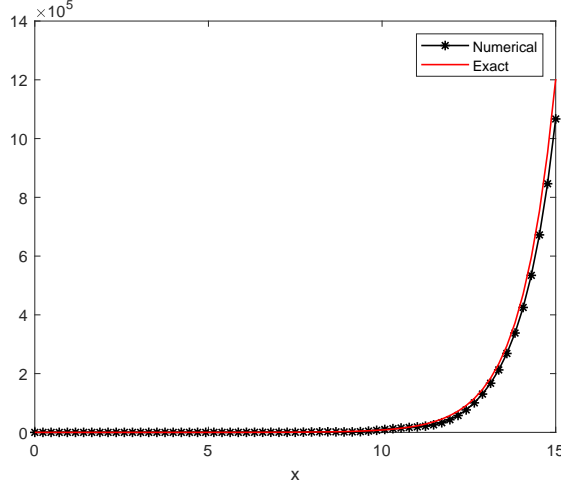


Fig. 2: Numerical and exact solutions for the convection equation with inflow boundary condition

## 4 Heat equation with Dirichlet or Neumann boundary conditions

In this section, we demonstrate how to solve parabolic PDEs with quantum simulations. Toward this end, we consider the linear heat equation

$$\begin{cases} u_t(\mathbf{x}, t) = \Delta u(\mathbf{x}, t) & \text{in } \Omega := (a, b)^d, \quad 0 < t < 1, \\ u(\mathbf{x}, 0) = u_0(\mathbf{x}), \\ u(\cdot, t) = 0 & \text{on } \partial\Omega, \end{cases}$$

where  $u_0(\mathbf{x})$  is the initial data. For periodic boundary conditions, one can refer to the detailed paper [JLY22b] on the Schrödingerisation approach, where the Fourier spectral approach is used to discretise both the spatial and the auxiliary variables. For other types of boundary conditions, we consider the finite difference discretisation for the spatial domain and use the spectral discretisation for the auxiliary variable.

Let us first consider the Dirichlet boundary conditions in 1D. The central difference discretisation gives

$$\frac{d}{dt}u_j(t) = \frac{u_{j-1}(t) - 2u_j(t) + u_{j+1}(t)}{\Delta x^2}, \quad j = 1, \dots, N_x - 1. \quad (4.1)$$

Let  $\mathbf{u}(t) = [u_1(t), \dots, u_{N_x-1}(t)]^T$ . One gets the system (2.2) with

$$A = \frac{1}{\Delta x^2} \begin{bmatrix} -2 & 1 & & & \\ 1 & -2 & \ddots & & \\ & \ddots & \ddots & \ddots & \\ & & \ddots & -2 & 1 \\ & & & 1 & -2 \end{bmatrix}_{(N_x-1) \times (N_x-1)}, \quad \mathbf{b}(t) = \frac{1}{\Delta x^2} \begin{bmatrix} u_0(t) \\ 0 \\ \vdots \\ 0 \\ u_{N_x}(t) \end{bmatrix}.$$

For  $d$  dimensions, the solution vector is defined by

$$\mathbf{u}_{h,d} = \sum_{j_1, \dots, j_d=1}^{N_x-1} u_{j_1, \dots, j_d} |j_1, \dots, j_d\rangle.$$

The corresponding coefficient matrix and right-hand vector in  $d$  dimensions will be replaced by

$$A_{h,d} = \underbrace{A \otimes I \otimes \cdots \otimes I}_{d \text{ matrices}} + I \otimes A \otimes \cdots \otimes I + \cdots + I \otimes I \otimes \cdots \otimes A \quad (4.2)$$

and

$$\mathbf{b}_{h,d}(t) = \frac{1}{\Delta x^2} \sum_{k=1}^d (\mathbf{u}_{0,k} + \mathbf{u}_{N_x,k}),$$

where

$$\begin{aligned} \mathbf{u}_{0,k} &= \sum_{j_i=1, i \neq k}^{N_x-1} u_{j_1, \dots, 0, \dots, j_d} |j_1, \dots, 1, \dots, j_d\rangle, \\ \mathbf{u}_{N_x,k} &= \sum_{j_i=1, i \neq k}^{N_x-1} u_{j_1, \dots, N_x, \dots, j_d} |j_1, \dots, N_x - 1, \dots, j_d\rangle. \end{aligned}$$

Here we present a numerical test. In the implementation, the initial and boundary values are chosen such that the exact solution is given by  $u(t, x) = e^{-\pi^2 t} \sin(\pi x)$ . As analyzed in the previous section, the associated waves move from right to left with speed

$$s_j = -\lambda_j \left( \frac{A + A^T}{2} \right) = \frac{4}{\Delta x^2} \sin^2 \frac{j\pi}{2N_x}, \quad j = 1, 2, \dots, N_x - 1$$

when  $\mathbf{b}(t) = \mathbf{0}$  is assumed. The fastest speed can be chosen as  $s_* = 4/\Delta x^2$ . To reduce the computational cost in the  $p$ -direction on a classical computer, as discussed in the preceding section, we take a relatively large spatial domain  $[a, b] = [0, 10]$ .

Considering the exponentially decreasing factor  $e^{-\pi^2 t}$  in the exact solution, we choose the evolution time  $T = 1/\pi^2$ . We also choose  $N_x - 1 = N_p = 64$ . Other parameters are the same as for the convection equation. The estimated  $L = -18.1233$ . The result at  $t = T$  is shown in Fig. 3.

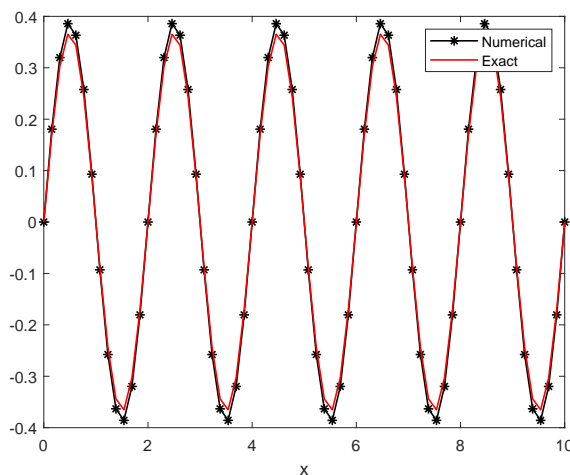


Fig. 3: Numerical and exact solutions for the heat equation with Dirichlet boundary conditions

We next consider the heat equation with the mixed boundary conditions:

$$u(t, a) = g(t), \quad u_x(t, b) = h(t).$$



## 5.1 The linear advection equation

We are concerned with a hyperbolic equation with discontinuous coefficients — a simple interface problem in the following form:

$$\begin{cases} \partial_t u + \nabla \cdot (c(x)u) = 0, & t > 0, x \in (-a, a)^d, \\ u(0, x) = u_0(x), & x \in [-a, a]^d, \end{cases} \quad (5.1)$$

where  $a > 0$  is a constant and  $c(x) = [c_1(x), \dots, c_d(x)]^T$  is a vector for fixed  $x = (x_1, \dots, x_d)$ . We assume that  $c(x)$  is piecewise constant in the  $x_1$ -direction:

$$c_i(x) = \begin{cases} c^- > 0, & x_1 < 0 \\ c^+ > 0, & x_1 > 0 \end{cases}, \quad i = 1, \dots, d.$$

The above equation arises in modeling wave propagation through interfaces with jumps in  $c(x)$  corresponding to interfaces between different media. For such a problem an interface condition is needed at  $x_1 = 0$ :

$$u(t, x^+) = \rho u(t, x^-), \quad (5.2)$$

where  $x^\pm$  represents the right and left limits in the  $x_1$ -direction,  $\rho = 1$  corresponds to the continuity of mass  $u$  or  $\rho = c^-/c^+$  for the continuity of flux  $cu$  [Jin09, WJ08].

In the following, we only consider the 1-D case. The exact solution of (5.1) with the interface condition (5.2) can be constructed following characteristics [WJ08], given by

$$u(t, x; u_0) = \begin{cases} u_0(x - c^-t), & x < 0, \\ \rho u_0(\frac{c^-}{c^+}x - c^-t), & 0 < x < c^+t, \\ u_0(x - c^+t), & x > c^+t. \end{cases}$$

Since the wave moves from left to right, we impose the boundary condition on the left endpoint.

When numerically solving (5.1), the most natural approach is to build the interface condition (5.2) into the numerical flux, as was proposed in [WJ08]. Let the uniform spatial mesh be  $x_j$ , where  $j = -N_x, \dots, -1, 0, 1, \dots, N_x$  and  $\Delta x = a/N_x$  is the mesh size. Since  $c^\pm > 0$ , one can apply the upwind scheme for  $x \leq 0$  and  $x > \Delta x$ :

$$\begin{cases} \frac{du_j}{dt} = -c^- \frac{u_j(t) - u_{j-1}(t)}{\Delta x}, & j = -(N_x - 1), \dots, 0, \\ \frac{du_j}{dt} = -c^+ \frac{u_j(t) - u_{j-1}(t)}{\Delta x}, & j = 2, \dots, N_x. \end{cases}$$

Note that in the above scheme  $u_0$  is the left limit of  $u$  at the interface. For  $j = 1$ , the continuity of  $cu$  gives

$$\frac{du_1}{dt} = -\frac{c^+u_1(t) - c^-u_0(t)}{\Delta x}, \quad j = 1.$$

Let  $\mathbf{u}(t) = [u_{-(N_x-1)}(t), \dots, u_{N_x}(t)]^T$ . One can collect the above equations as the system (2.2)



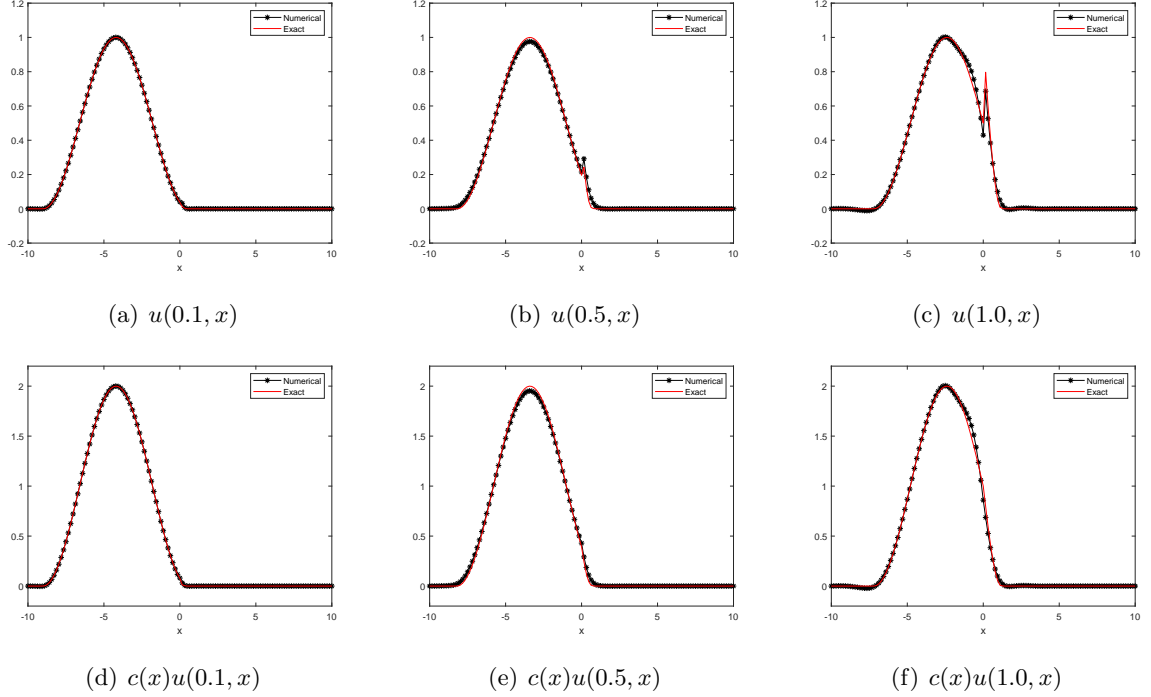


Fig. 5: Numerical and exact solutions for the interface problem. Top: the solution  $u(T, x)$ ; Bottom: the flux  $c(x)u(T, x)$ .

with the jump condition on a moving interface  $\alpha(t) \in (a, b)$ :

$$\begin{aligned} [u]_{x=\alpha(t)} &= u^+ - u^- = 0, \\ [\beta u_x]_{x=\alpha(t)} &= \beta^+ u^+ - \beta^- u^- = 0. \end{aligned}$$

The interface separates  $\Omega$  into the left and right subdomains  $\Omega^-(t)$  and  $\Omega^+(t)$ . For simplicity, we assume  $\beta(t, x)$  is a piecewise constant function:

$$\beta(t, x) = \begin{cases} \beta^- > 0, & x \in \Omega^-(t), \\ \beta^+ > 0, & x \in \Omega^+(t). \end{cases}$$

In the following, we assume that  $t$  is fixed and simply write  $\alpha(t)$  as  $\alpha$ . In this case one can apply the immersed interface method in [LL94] for the spatial discretisation. Let the uniform grid in the interval  $[a, b]$  be

$$a = x_0 < x_1 < \dots < x_N = b, \quad x_i = a + ih, \quad h = (b - a)/N.$$

The goal is to develop semi-discrete finite difference equations of the form

$$\frac{d}{dt} u_i(t) = \gamma_{i,1}(t) u_{i-1}(t) + \gamma_{i,2}(t) u_i(t) + \gamma_{i,3}(t) u_{i+1}(t) + f_i, \quad i = 1, 2, \dots, N-1,$$

with second-order accurate approximation to  $u$  at the uniform grid points. Note that  $\gamma_{i,1}$ ,  $\gamma_{i,2}$  and  $\gamma_{i,3}$  depend on the time variable because of the moving interface.

If we impose the Dirichlet boundary conditions, then the semi-discrete system can be written as

$$\frac{d}{dt} \mathbf{u}(t) = A(t) \mathbf{u}(t) + \mathbf{b}(t),$$

where  $\mathbf{u}(t) = [u_1(t), \dots, u_{N-1}(t)]^T$ , and

$$A(t) = \begin{bmatrix} \gamma_{1,2} & \gamma_{1,3} & & & \\ \gamma_{2,1} & \ddots & \ddots & & \\ & \ddots & \ddots & \gamma_{N-2,3} & \\ & & \gamma_{N-1,1} & \gamma_{N-1,2} & \end{bmatrix}, \quad \mathbf{b}(t) = \begin{bmatrix} \gamma_{1,1}u_0(t) + f_1 \\ f_2 \\ \vdots \\ f_{N-2} \\ \gamma_{N-1,3}u_N(t) + f_{N-1} \end{bmatrix}.$$

Let  $\alpha$  fall between  $x_k$  and  $x_{k+1}$ , i.e.,  $x_k \leq \alpha < x_{k+1}$  (note that  $k$  depends on  $t$ ). For  $i \neq k, k+1$  the solution can be viewed as a smooth function in  $[x_k, x_{k+1}]$  and one can use the standard approximation

$$\frac{1}{\Delta x^2} \left( \beta_{i+1/2}(u_{i+1} - u_i) - \beta_{i-1/2}(u_i - u_{i-1}) \right)$$

for  $(\beta u_x)_x$  at  $x = x_i$ , where  $\beta_{i\pm 1/2} = \beta(x_{i\pm 1/2})$ . In this case one has

$$\gamma_{i,1} = \beta_{i-1/2}/h^2, \quad \gamma_{i,2} = -(\beta_{i-1/2} + \beta_{i+1/2})/h^2, \quad \gamma_{i,3} = \beta_{i+1/2}/h^2.$$

For  $i = k, k+1$ , following [LL94], we take

$$\begin{aligned} \gamma_{k,1} &= (\beta^- - [\beta](x_k - \alpha)/h)/D_k, & \gamma_{k+1,1} &= \beta^-/D_{k+1}, \\ \gamma_{k,2} &= (-2\beta^- + [\beta](x_{k-1} - \alpha)/h)/D_k, & \gamma_{k+1,2} &= (-2\beta^+ + [\beta](x_{k+2} - \alpha)/h)/D_{k+1}, \\ \gamma_{k,3} &= \beta^+/D_k, & \gamma_{k+1,3} &= (\beta^+ - [\beta](x_{k+1} - \alpha)/h)/D_{k+1}, \end{aligned}$$

where

$$D_k = h^2 + [\beta](x_{k-1} - \alpha)(x_k - \alpha)/2\beta^-, \quad D_{k+1} = h^2 - [\beta](x_{k+2} - \alpha)(x_{k+1} - \alpha)/2\beta^+.$$

It is easy to show that  $D_k$  and  $D_{k+1}$  are positive when  $\beta > 0$ .

We implemented this model with the initial and boundary value functions chosen such that the exact solution is

$$u(t, x) = \begin{cases} \left( (x - \alpha(t))^2 + \frac{1}{\beta^-} \right) e^x, & x \in \Omega^-(t), \\ \left( (x - \alpha(t))^2 + \frac{1}{\beta^+} \right) e^x + \left( \frac{1}{\beta^-} - \frac{1}{\beta^+} \right) e^{\alpha(t)}, & x \in \Omega^+(t), \end{cases}.$$

We set  $\alpha(t) = \frac{1}{2}t + \frac{1}{4}$  and  $\beta^- = 1$  and  $\beta^+ = 2$ . The backward Euler method is used for the temporal discretisation. The spatial domain is taken as  $[0, 10]$ . We set  $N = 100$  and  $N_t = 100$  and display the solutions at  $t = 1$  in Fig. 6, from which one can see that the Schrödingerisation approach gives the desired solution for the problem with interface varying in time.

## 6 Geometric optics problems with partial transmissions and reflections

In this section we are concerned with the quantum simulation of geometric optics problems when both transmissions and reflections occur at the interface.

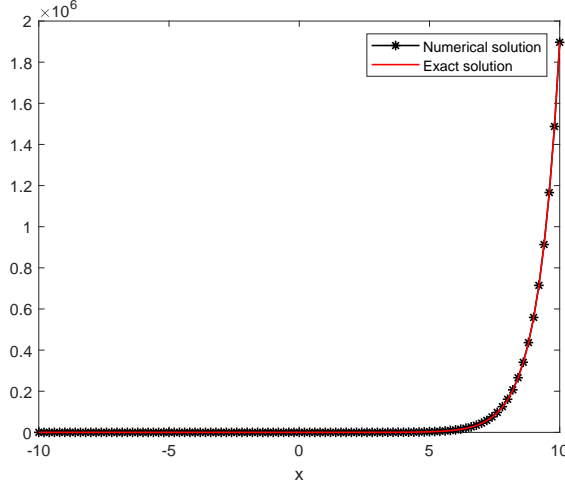


Fig. 6: Numerical and exact solutions for the Stefan problem

## 6.1 The geometric optics problem

### 6.1.1 The Hamilton-Jacobi equation for the geometric optics

We consider the linear scalar wave equation in the high frequency regime,

$$w_{tt} - c(x)^2 \Delta w = 0, \quad x \in \mathbb{R}^d, \quad (6.1)$$

where  $c(x)$  is the local speed of wave propagation of the medium, or the reciprocal of the index of refraction. When the waves are of high frequency, (6.1) is a multiscale problem, where the small scale is given by the wavelength over, for example, the overall size of the computational domain. For sufficiently high frequencies, direct numerical simulation is no longer feasible. Numerical methods based on approximations of (6.1) are needed.

The derivation of the geometrical optics equations in the linear case follows if one assumes a series expansion of the form

$$w(t, x) = e^{i\omega S(t, x)} \sum_{k=0}^{\infty} A_k(t, x) (i\omega)^{-k}. \quad (6.2)$$

Plugging this expression into (6.1) and collecting terms of the same order in  $\omega$ , one obtains separate equations for the unknown dependent variables in (6.2). The  $\mathcal{O}(\omega^2)$  terms give the equation for the phase function  $S$ , which satisfies the Hamilton-Jacobi-type eikonal equation [ER03]

$$\partial_t \phi + c(x) |\nabla S| = 0. \quad (6.3)$$

Hamilton-Jacobi equations (HJE) take the following general form

$$\begin{aligned} \partial_t S + H(\nabla S, x) &= 0, \\ S(0, x) &= S_0(x) \end{aligned} \quad (6.4)$$

with  $t \in \mathbb{R}^+$ ,  $x \in \mathbb{R}^d$ ,  $S(t, x) \in \mathbb{R}$ . For the geometric optics equation (6.3), the associated Hamiltonian is given by

$$H(\xi, x) = c(x) |\xi|. \quad (6.5)$$

### 6.1.2 The Liouville representation for the Hamilton-Jacobi equation

Define  $u = \nabla S \in \mathbb{R}^d$ . Then  $u$  solves a hyperbolic system of conservation laws in gradient form:

$$\begin{aligned}\partial_t u + \nabla H(u, x) &= 0, \\ u(0, x) &= \nabla S_0(x).\end{aligned}\tag{6.6}$$

Ref. [JL22] constructed quantum algorithms to compute physical observables of this nonlinear problem, which is based on an exact mapping between nonlinear and linear PDEs using the level set method [JO03]. This approach is referred to as the linear representation approach, and it is based on an *exact* map from a nonlinear PDE to a linear one thus *no* physical information is lost, while other approaches are based on linear approximations that use *truncation* to linearize the problem so they are *not* the same physical problem as the original nonlinear one. A more comprehensive discussion can be found in [JLY23], where the finite difference and spectral discretisations are discussed with periodic boundary conditions applied.

We follow the linear representation approach in [JL22]. The level set function  $\phi_i(t, x, p)$  can be defined by

$$\phi_i(t, x, \xi = u(t, x)) = 0,$$

where  $i = 1, \dots, d$  and  $x, \xi \in \mathbb{R}^d$ , and  $u(t, x)$  is the solution of Eq. (6.6). The *zero level set* of  $\phi$  is the set  $\{(t, x, p) | \phi_i(t, x, \xi) = 0\}$ . Since  $u(t, x)$  solves Eq. (6.6), one can show that  $\phi = (\phi_1, \dots, \phi_d) \in \mathbb{R}^d$  solves a (linear!) Liouville equation [JO03]

$$\partial_t \phi + \nabla_\xi H \cdot \nabla_x \phi - \nabla_x H \cdot \nabla_\xi \phi = 0.\tag{6.7}$$

The initial data can be chosen as

$$\phi_i(0, x, \xi) = \xi_i - u_i(0, x), \quad i = 1, \dots, d.\tag{6.8}$$

Then  $u$  can be recovered from the intersection of the zero level sets of  $\phi_i$  ( $i = 1, \dots, d$ ), namely

$$u(t, x) = \{\xi(t, x) | \phi_i(t, x, \xi) = 0, i = 1, \dots, d\}.$$

To retrieve physical observables (and to avoid finding the zero level set of  $\phi$  which is challenging) later, [JL22] proposed to solve for  $f$ , defined by the following problem

$$\begin{aligned}\partial_t f + \nabla_\xi H \cdot \nabla_x f - \nabla_x H \cdot \nabla_\xi f &= 0, \\ f(0, x, \xi) &= \prod_{i=1}^d \delta(\xi_i - u_i(0, x)),\end{aligned}\tag{6.9}$$

whose analytical solution is  $f(t, x, \xi) = \delta(\phi(t, x, \xi))$ . We have thus transformed a  $(d+1)$ -dimensional nonlinear Hamilton-Jacobi PDE to a  $(2d+1)$ -dimensional *linear* PDE – the Liouville equation, without *any* approximations or constraints on the nonlinearity. The mapping is *exact*, but at the expense of doubling the spatial dimension.

For geometric optics, the Liouville equation can be written as

$$f_t + c(x) \frac{\xi}{|\xi|} \cdot \nabla_x f - |\xi| \nabla_x c \cdot \nabla_\xi f = 0. \quad (6.10)$$

The bicharacteristics of the Liouville equation (6.10) satisfy the Hamiltonian system:

$$\frac{dx}{dt} = c(x) \frac{\xi}{|\xi|}, \quad \frac{d\xi}{dt} = -|\xi| \nabla_x c. \quad (6.11)$$

In particular, the 1-D Liouville equation is

$$f_t + c(x) \text{sign}(\xi) f_x - c_x |\xi| f_\xi = 0,$$

where  $c(x) > 0$  may be discontinuous at the interface between two media.

### 6.1.3 The condition for transmissions and reflections at the interface

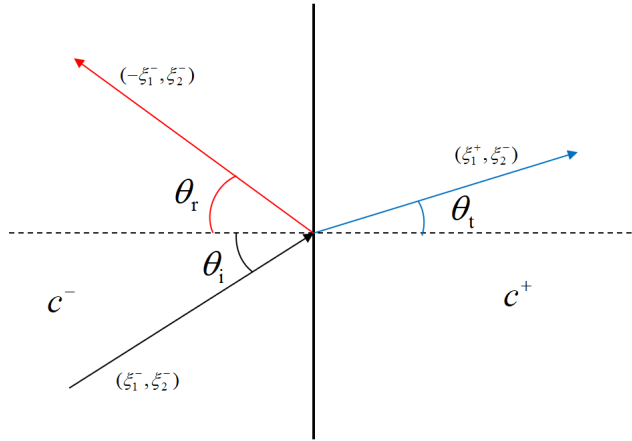


Fig. 7: Wave transmission and reflection at an interface

In geometrical optics, when a wave moves with its density distribution governed by the Liouville equation, its Hamiltonian  $H = c|\xi|$  should be preserved across the interface

$$H(x^+, \xi^+) = H(x^-, \xi^-) \quad \text{or} \quad c^- |\xi^-| = c^+ |\xi^+|, \quad (6.12)$$

where the superscripts  $\pm$  represent the right and left limits of the quantity at the interface. Let us consider a 2-D example. When a plane wave hits a flat vertical interface as shown in Fig. 7, the Hamiltonian preserving condition (6.12) is equivalent to Snell's law of refraction

$$\frac{\sin \theta_i}{c^-} = \frac{\sin \theta_t}{c^+},$$

and the reflection law

$$\theta_r = \theta_i,$$

where  $\theta_i$ ,  $\theta_t$  and  $\theta_r$  stand for angles of incident, transmitted and reflected waves. Let  $\xi = (\xi_1, \xi_2)$ . Assume that the incident wave has a velocity  $(\xi_1^-, \xi_2^-)$  to the left side of the interface, with  $\xi_1^- > 0$ . Since the interface is vertical ( $\partial_y c = 0$ ), the characteristic of  $\xi$  in (6.11) implies that  $\xi_2$  is not

changed when the wave crosses the interface. When  $c^- > c^+$ , the wave can partially transmit and partially be reflected. In this case, the local wave speed decreases, so the wave will cross the interface and increase its  $\xi$  value in order to maintain a constant Hamiltonian. The preserving condition (6.12) implies

$$\xi_1^+ = \sqrt{\rho^2(\xi_1^-)^2 + (\rho^2 - 1)(\xi_2^-)^2}, \quad \rho = c^-/c^+.$$

As a linear hyperbolic equation, the solution to the Liouville equation (6.10), can be obtained by the method of characteristics. Namely, the density distribution  $f$  remains a constant along a bicharacteristic. However, when partial transmissions and reflections are considered, this is no longer valid, since  $f$  needs to be determined from two bicharacteristics, one accounting for the transmission and the other for reflection. Ref. [JW06b] uses the following condition at the interface:

$$f(t, x^+, \xi^+) = \alpha_T f(t, x^-, \xi^-) + \alpha_R f(t, x^+, -\xi^+), \quad (6.13)$$

where  $\alpha_T, \alpha_R \in [0, 1]$  are the transmission and reflection coefficients, satisfying  $\alpha_T + \alpha_R = 1$ , and  $x^+ = x^-$  (for a sharp interface). Note that for a complete transmission,  $f(t, x^+, \xi^+) = f(t, x^-, \xi^-)$ , while for a complete reflection,  $f(t, x^+, \xi^+) = f(t, x^-, -\xi^-)$  and  $\xi^- = \xi^+$ . For partial transmissions and reflections  $\alpha_R, \alpha_T \in (0, 1)$ .

## 6.2 The Hamiltonian-preserving scheme

### 6.2.1 The numerical flux

We now describe the Hamiltonian-preserving finite difference scheme proposed in [JW06a, JW06b] for the 1-D Liouville equation

$$f_t + c(x)\text{sign}(\xi)f_x - c_x|\xi|f_\xi = 0,$$

where  $c(x) > 0$  may be discontinuous.

We use a uniform mesh with grid points at  $x_{i+\frac{1}{2}}$ ,  $i = 0, 1, \dots, N$  in the  $x$ -direction and  $\xi_{j+\frac{1}{2}}$ ,  $j = 0, 1, \dots, M$  in the  $\xi$ -direction. The cells are centered at  $(x_i, \xi_j)$  for  $1 \leq i \leq N$  and  $1 \leq j \leq M$ , where  $x_i = \frac{1}{2}(x_{i-\frac{1}{2}} + x_{i+\frac{1}{2}})$  and  $\xi_j = \frac{1}{2}(\xi_{j-\frac{1}{2}} + \xi_{j+\frac{1}{2}})$ . The cell average of  $f$  is defined by

$$f_{ij} = \frac{1}{\Delta x \Delta \xi} \int_{x_{i-\frac{1}{2}}}^{x_{i+\frac{1}{2}}} \int_{\xi_{j-\frac{1}{2}}}^{\xi_{j+\frac{1}{2}}} f(t, x, \xi) d\xi dx.$$

Assume that the discontinuous points of the wave speed  $c$  are located at the grid points. Let the right and left limits of  $c(x)$  at point  $x_{i+\frac{1}{2}}$  be  $c_{i+\frac{1}{2}}^+$  and  $c_{i+\frac{1}{2}}^-$ , respectively. We define the average wave speed as  $c_i = \frac{1}{2}(c_{i-\frac{1}{2}}^- + c_{i+\frac{1}{2}}^+)$ . The flux splitting technique is adopted here. The semi-discrete scheme reads

$$\frac{d}{dt} f_{ij} + \frac{c_i \text{sign}(\xi_j)}{\Delta x} (f_{i+\frac{1}{2}, j}^+ - f_{i-\frac{1}{2}, j}^-) - \frac{c_{i+\frac{1}{2}}^+ - c_{i-\frac{1}{2}}^-}{\Delta x \Delta \xi} |\xi_j| (f_{i, j+\frac{1}{2}} - f_{i, j-\frac{1}{2}}) = 0 \quad (6.14)$$

for  $1 \leq i \leq N$  and  $1 \leq j \leq M$ , where the numerical fluxes  $f_{i, j+\frac{1}{2}}$  in the  $\xi$ -direction are defined using the upwind discretisation, that is,

$$f_{i, j+\frac{1}{2}} - f_{i, j-\frac{1}{2}} = \begin{cases} f_{ij} - f_{i, j-1}, & c_\xi \geq 0 \\ f_{i, j+1} - f_{ij}, & c_\xi < 0 \end{cases}, \quad c_\xi = -\frac{c_{i+\frac{1}{2}}^+ - c_{i-\frac{1}{2}}^-}{\Delta x \Delta \xi} |\xi_j|.$$

Since the characteristics of the Liouville equation may be different on the two sides of the interface, the corresponding numerical fluxes should also be different. The essential part of the algorithm is to define the split numerical fluxes  $f_{i+\frac{1}{2},j}^\pm$  at the cell interface by utilizing the interface condition (6.13).

Assume  $c$  is discontinuous at  $x_{i+\frac{1}{2}}$ . Consider the case  $\xi_j > 0$ . Since the wave moves from left to right in  $[x_i, x_{i+\frac{1}{2}}]$ , we can define the interface value  $f_{i+\frac{1}{2},j}^+ = f_{ij}$  using the upwind approximation. According to the interface condition (6.13),

$$f_{i+\frac{1}{2},j}^- = \alpha_T f(t, x_{i+\frac{1}{2}}^+, \xi_j^+) + \alpha_R f(t, x_{i+\frac{1}{2}}^-, -\xi_j^-),$$

where  $\xi_j^+$  is obtained from  $\xi_j^- = \xi_j$  from (6.12). Noting that  $\xi_j^+$  may not be a grid point, we have to define it approximately. One can first locate the two cell centers that bound this velocity, and then use linear interpolation to evaluate the needed numerical flux at  $\xi_j^+$ . The case  $\xi_j < 0$  can be treated similarly.

The algorithm of computing the numerical flux is summarized in Algorithm 1.

---

**Algorithm 1** Computation of the numerical flux in  $x$ -direction

---

Case 1:  $\xi_j > 0$ .

- $f_{i+\frac{1}{2},j}^+ = f_{ij}$ ,  $\xi' = \frac{c_{i+\frac{1}{2}}^-}{c_{i+\frac{1}{2}}^+} \xi_j$ .
- If  $\xi_k \leq \xi' < \xi_{k+1}$  for some  $k$ , then

$$a_R = \left( \frac{c_{i+\frac{1}{2}}^+ - c_{i+\frac{1}{2}}^-}{c_{i+\frac{1}{2}}^+ + c_{i+\frac{1}{2}}^-} \right)^2, \quad a_T = 1 - a_R,$$

$$f_{i+\frac{1}{2},j}^- = a_T \left( \frac{\xi_{k+1} - \xi'}{\Delta\xi} f_{i,k} + \frac{\xi' - \xi_k}{\Delta\xi} f_{i,k+1} \right) + a_R f_{i+1,k'},$$

where  $\xi_{k'} = -\xi_k$ .

Case 2:  $\xi_j < 0$ .

- $f_{i+\frac{1}{2},j}^- = f_{i+1,j}$ ,  $\xi' = \frac{c_{i+\frac{1}{2}}^+}{c_{i+\frac{1}{2}}^-} \xi_j$ .
- If  $\xi_k \leq \xi' < \xi_{k+1}$  for some  $k$ , then

$$a_R = \left( \frac{c_{i+\frac{1}{2}}^+ - c_{i+\frac{1}{2}}^-}{c_{i+\frac{1}{2}}^+ + c_{i+\frac{1}{2}}^-} \right)^2, \quad a_T = 1 - a_R,$$

$$f_{i+\frac{1}{2},j}^+ = a_T \left( \frac{\xi_{k+1} - \xi'}{\Delta\xi} f_{i+1,k} + \frac{\xi' - \xi_k}{\Delta\xi} f_{i+1,k+1} \right) + a_R f_{i,k'},$$

where  $\xi_{k'} = -\xi_k$ .

---

## 6.2.2 The Schrödingerisation simulation

We consider the first example in [JW06b]. The discontinuous wave speed is given by

$$c(x) = \begin{cases} 0.6, & x < 0, \\ 0.2, & x > 0. \end{cases}$$

The initial data is

$$f(0, x, \xi) = \begin{cases} 1, & x < 0, \xi > 0, \sqrt{x^2 + 4\xi^2} < 1, \\ 1, & x > 0, \xi < 0, \sqrt{x^2 + \xi^2} < 1, \\ 0, & \text{otherwise.} \end{cases}$$

The exact solution for  $f$  at  $t = 1$  is given by

$$f(x, \xi, 1) = \begin{cases} \alpha^T, & 0 < x < 0.2, \quad \sqrt{1 - (0.2 - x)^2} < \xi < 1.5\sqrt{1 - (3x - 0.6)^2}, \\ 1, & 0 < x < 0.2, \quad 0 < \xi < \sqrt{1 - (0.2 - x)^2}, \\ 1, & 0 < x < 0.8, \quad -\sqrt{1 - (x + 0.2)^2} < \xi < 0, \\ 1, & -0.4 < x < 0, \quad 0 < \xi < \frac{1}{2}\sqrt{1 - (x - 0.6)^2}, \\ 1, & -0.6 < x < 0, \quad -\frac{1}{3}\sqrt{1 - (\frac{x}{3} + 0.2)^2} < \xi < 0, \\ \alpha^R, & -0.6 < x < 0, \quad -\frac{1}{2}\sqrt{1 - (x + 0.6)^2} < \xi < -\frac{1}{3}\sqrt{1 - (\frac{x}{3} + 0.2)^2}, \\ 0, & \text{otherwise.} \end{cases}$$

In the implementation, we choose a large enough domain that contains the supports of the initial and final solutions. For this example, one can take it as  $[-1.5, 1.5]^2$ . To save the computational cost in the  $p$ -direction, where  $p$  is the auxiliary variable for the Schrödingerisation approach, we set it as  $[-4, 4]^2$ . For simplicity, we use the forward Euler method to iteratively get the updated solution. We take  $N = M = 200$  and  $N_t = 1000$ , where  $N_t$  is the number of steps for time discretisation. The numerical result is displayed in Fig. 8. Due to the first-order accuracy in  $x, \xi, p$  and  $t$ , the numerical solution has some smearing across the discontinuities, which is expected and can be improved by using more grid points or using higher order approximations. We remark that for the direct upwind discretisation, the CFL condition requires the time step to satisfy  $\Delta t = \mathcal{O}(\Delta x \Delta \xi)$ . However, the Hamiltonian preserving scheme allows a time step  $\Delta t = \mathcal{O}(\Delta x, \Delta \xi)$ .

## 7 Conclusion

Quantum simulations for time-dependent or independent boundary value problems of partial differential equations are quite difficult because the ODE system resulting from spatial discretisations is not necessarily a Hamiltonian system. Spatial discretisation of the boundary condition, like the Dirichlet boundary condition for example, could also give rise to an inhomogeneous term in the system ( $\mathbf{b} \neq \mathbf{0}$  in (2.2)). Our Schrödingerisation approach combined with the augmentation technique resolves this problem in a generic and efficient way as shown in [JLLY23] and this work.

In this article, we extend the Schrödingerisation approach [JLY22a, JLY22b] for quantum simulations of PDEs to problems with physical boundary or interface conditions. While a quantum

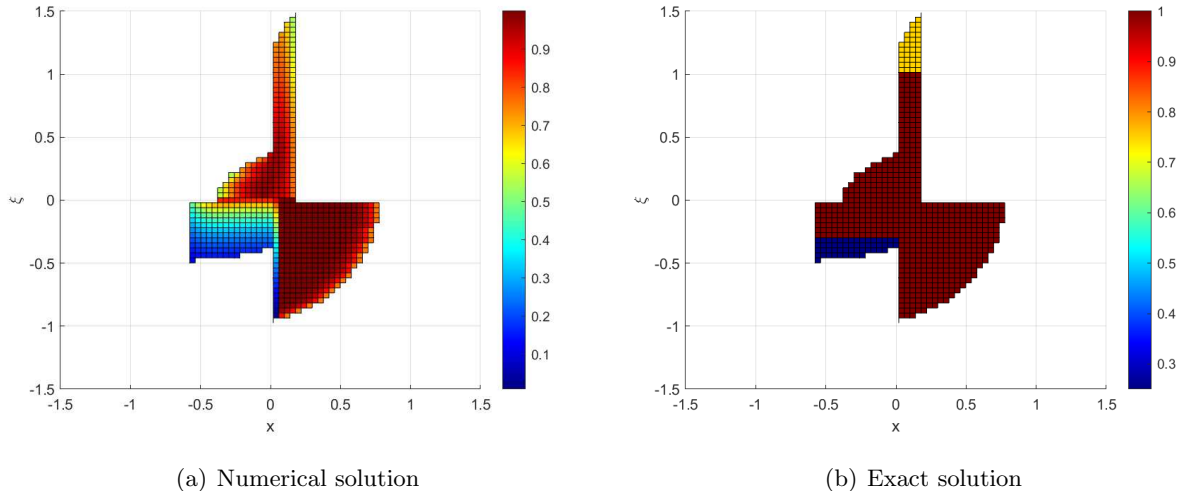


Fig. 8: Snapshots of the nonzero part of the solutions for the Hamiltonian preserving scheme.

dynamics with physical boundary or interface conditions is no longer a Hermitian Hamiltonian system, the Schrödingerisation approach makes it so in a simple fashion. We give the implementation details for these problems. The numerical experiments validate this approach, demonstrating that the Schrödingerised systems yield the same results as the original dynamics. This further extends the Schrödingerisation techniques toward real applications of partial differential equations which most often are coupled with boundary or interface conditions.

## Acknowledgements

SJ was partially supported by the NSFC grant No. 12031013, the Shanghai Municipal Science and Technology Major Project (2021SHZDZX0102), and the Innovation Program of Shanghai Municipal Education Commission (No. 2021-01-07-00-02-E00087). NL acknowledges funding from the Science and Technology Program of Shanghai, China (21JC1402900). YY was partially supported by China Postdoctoral Science Foundation (no. 2022M712080). XL is supported by a Seed Grant from the Institute of Computational and Data Science (ICDS) at Penn State.

## References

- [ALWZ22] D. An, J. Liu, D. Wang, and Q. Zhao. A theory of quantum differential equation solvers: limitations and fast-forwarding. *arXiv:2211.05246v1*, 2022.
- [BCOW17] D. W. Berry, A. M. Childs, A. Ostrander, and G. Wang. Quantum algorithm for linear differential equations with exponentially improved dependence on precision. *Comm. Math. Phys.*, 356(3):1057–1081, 2017.
- [BCS<sup>+</sup>20] D. W. Berry, A. M. Childs, Y. Su, X. Wang, and N. Wiebe. Time-dependent Hamiltonian simulation with  $l^1$ -norm scaling. *Quantum*, 4:254, 2020.

- [Ber14] D. W. Berry. High-order quantum algorithm for solving linear differential equations. *J. Phys. A: Math. Theor.*, 47(10):105301, 17 pp., 2014.
- [CAS<sup>+</sup>21] P. C. S. Costa, D. An, Y. A. Sanders, Y. Su, R. Babbush, and D. W. Berry. Optimal scaling quantum linear systems solver via discrete adiabatic theorem. *arXiv:2111.08152*, 2021.
- [CJO19] P. C. S. Costa, S. Jordan, and A. Ostrander. Quantum algorithm for simulating the wave equation. *Phys. Rev. A*, 99:012323, 22 pp., 2019.
- [CKS17] A. M. Childs, R. Kothari, and R. D. Somma. Quantum algorithm for systems of linear equations with exponentially improved dependence on precision. *SIAM J. Comput.*, 46(6):1920–1950, 2017.
- [CL20] A. W. Childs and J. Liu. Quantum spectral methods for differential equations. *Comm. Math. Phys.*, 375(2):1427–1457, 2020.
- [CLO21] A. M. Childs, J. P. Liu, and A. Ostrander. High-precision quantum algorithms for partial differential equations. *Quantum*, 5:574, 2021.
- [CPP<sup>+</sup>13] Y. Cao, A. Papageorgiou, I. Petras, et al. Quantum algorithm and circuit design solving the Poisson equation. *New J. Phys.*, 15:013021, 2013.
- [ER03] B. Engquist and O. Runborg. Computational high frequency wave propagation. *Acta Numer.*, 12:181–266, 2003.
- [ESP19] A. Engel, G. Smith, and S. E. Parker. Quantum algorithm for the Vlasov equation. *Phys. Rev. A*, 100:062315, Dec 2019.
- [GJL22] F. Golse, S. Jin, and N. Liu. Quantum algorithms for uncertainty quantification: application to partial differential equations. *arXiv:2209.11220*, 2022.
- [HHL09] A. W. Harrow, A. Hassidim, and S. Lloyd. Quantum algorithm for linear systems of equations. *Phys. Rev. Lett.*, 103(15):150502, 4 pp., 2009.
- [Jin09] S. Jin. Numerical methods for hyperbolic systems with singular coefficients: well-balanced scheme, Hamiltonian preservation, and beyond. In *Hyperbolic Problems: Theory, Numerics and Applications, Part 1: Plenary & Invited Talks*, volume 67, pages 93–104. Amer. Math. Soc., Proc. Sympos. Appl. Math., 2009.
- [JL22] S. Jin and N. Liu. Quantum algorithms for computing observables of nonlinear partial differential equations. *arXiv:2202.07834*, 2022.
- [JL23] S. Jin and N. Liu. Quantum simulation of discrete linear dynamical systems and simple iterative methods in linear algebra via schrodingerisation. *arXiv preprint arXiv:2304.02865*, 2023.

- [JLLY23] S. Jin, X. Li, N. Liu, and Y. Yu. Quantum simulation for quantum dynamics with artificial boundary conditions. *arXiv: 2304.00667*, 2023.
- [JLY22a] S. Jin, N. Liu, and Y. Yu. Quantum simulation of partial differential equations via Schrödingerisation. *arXiv:2212.13969*, 2022.
- [JLY22b] S. Jin, N. Liu, and Y. Yu. Quantum simulation of partial differential equations via Schrödingerisation: technical details. *arXiv:2212.14703*, 2022.
- [JLY22c] S. Jin, N. Liu, and Y. Yu. Time complexity analysis of quantum difference methods for linear high dimensional and multiscale partial differential equations. *J. Comput. Phys.*, 471:111641, 2022.
- [JLY23] S. Jin, N. Liu, and Y. Yu. Time complexity analysis of quantum algorithms via linear representations for nonlinear ordinary and partial differential equations. *J. Comput. Phys.*, 487:112149, 2023.
- [JO03] S. Jin and S. Osher. A level set method for the computation of multivalued solutions to quasi-linear hyperbolic PDEs and Hamilton-Jacobi equations. *Commun. Math. Sci.*, 1(3):575–591, 2003.
- [JW05] S. Jin and X. Wen. Hamiltonian-preserving schemes for the Liouville equation with discontinuous potentials. *Commun. Math. Sci.*, 3(3):285–315, 2005.
- [JW06a] S. Jin and X. Wen. A Hamiltonian-preserving scheme for the Liouville equation of geometrical optics with discontinuous local wave speeds. *J. Comput. Phys.*, 214(2):672–697, 2006.
- [JW06b] S. Jin and X. Wen. A Hamiltonian-preserving scheme for the Liouville equation of geometrical optics with partial transmissions and reflections. *SIAM J. Numer. Anal.*, 44(5):1801–1828, 2006.
- [LL94] R. J. Leveque and Z. Li. The immersed interface method for elliptic equations with discontinuous coefficients and singular sources. *SIAM J. Numer. Anal.*, 31(4):1019–1044, 1994.
- [LMS20] N. Linden, A. Montanaro, and C. Shao. Quantum vs. classical algorithms for solving the heat equation. *arXiv:2004.06516*, 2020.
- [LW18] G. Low and N. Wiebe. Hamiltonian simulation in the interaction picture. *arXiv preprint arXiv:1805.00675*, 2018.
- [MP16] A. Montanaro and S. Pallister. Quantum algorithms and the finite element method. *Phys. Rev. A*, 93:032324, 14 pp., 2016.
- [Pes02] Charles S Peskin. The immersed boundary method. *Acta Numer.*, 11:479–517, 2002.
- [Rub71] LI Rubinshtein. *The Stefan Problem*, volume 27. American Mathematical Soc., 1971.

- [SS19] Y. Subasi and R. D. Somma. Quantum algorithms for systems of linear equations inspired by adiabatic quantum computing. *Phys. Rev. Lett.*, 122:060504, 2019.
- [WJ08] X. Wen and S. Jin. Covergence of an immersed interface upwind scheme for linear advection equations with piecewise constant coefficients I:  $L^1$ -error estimates. *J. Comput. Math.*, 26:1–22, 2008.
- [ZL97] C. Zhang and R. J. Leveque. The immersed interface method for acoustic wave equations with discontinuous coefficients. *Wave Motion*, 25(3):237–263, 1997.